Empirical and Physical Modeling of Self-Heating in Power AlGaN/GaN HEMTs

M. Bernardoni, N. Delmonte, R. Menozzi

Department of Information Engineering, University of Parma, Parco Area delle Scienze 181A, 43124 Parma, Italy
roberto.menozzi@unipr.it, Tel. +39-0521-905832

Keywords: ***Gallium nitride, thermal effects, thermal modeling modeling, reliability.***

Abstract

This work shows results of dynamic lumped-element (LE) thermal modeling of power AlGaN/GaN HEMTs. A realistic 3D structure including top-side metals, GaN-Si thermal boundary resistance, die-attach, and source via hole is modeled using a finite-element (FE) tool, and the results are used to develop simplified LE dynamic thermal models. We show that the LE models can match the FE data with excellent accuracy.

INTRODUCTION

Self-heating is among the most significant performance and reliability limiters for power devices and circuits. GaN-based HEMTs, today's most promising technology for microwave PAs, but rapidly emerging among high-power switches, too, are a case in point, since exploiting to the fullest the outstanding material properties necessitates thermal aspect to be carefully addressed in device design and manufacturing. While Finite Element (FE) simulation is a powerful physical modeling approach able to deal with large 3D structures made of different materials (with temperature-dependent thermal conductivities), and including top- and back-side features and boundary conditions, FE models can be computationally heavy and cannot be integrated in design suites, unlike lumped-element (LE) models.

In previous works, we proposed a hybrid approach, whereby LE 2D [1] or 3D [2] thermal networks representing physical models of the device are coupled with large-signal electro-thermal HEMT models for self-consistent simulation of the device DC and RF behavior including self-heating. This technique proved to be accurate enough, but becomes cumbersome for complex structures like large-periphery HEMTs for PAs, and when top metal lines and pads, as well as via holes etc., are to be included in the thermal model.

Therefore, in this work we explore and discuss an alternative modeling approach that uses very simple LE networks. We use FE simulation to validate the LE models.

FINITE-ELEMENT SIMULATIONS

Fig. 1 shows the HEMT structure we use as a test bench: it is the basic building block of a much larger power HEMT; the whole HEMT can be thought of as a periodic repetition of such blocks. Fig. 2 shows a blow-up of the HEMT surface, where the thin (blue) gate fingers can be discerned.

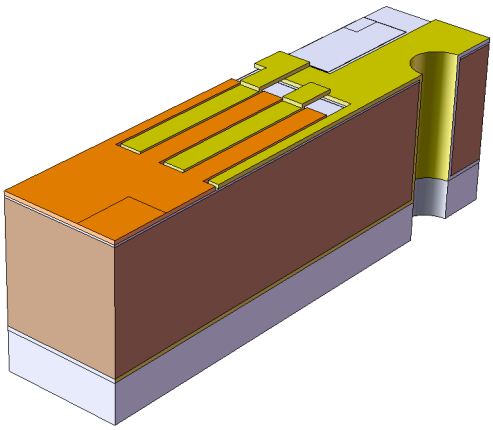

Fig. 1 The modeled structure, representing the building block of a large-periphery power AlGaN/GaN HEMT.

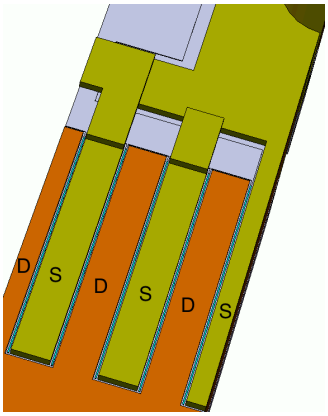

Fig. 2 A blow-up of Fig. 1, with drain and source fingers indicated as D and S, respectively.

The block is made of 5, 200 μm wide fingers (where heat is generated), abutting interdigitated source/drain regions. Metal lines and a source via hole are included in the model, as well as the bottom die-attach layer, (Fig. 1). We consider the case of Si substrate. GaN and Si thermal conductivities are temperature-dependent [4]. Thermal boundary resistance (TBR) is included between GaN and Si [5]. The details of the structure geometry and material properties are as follows:

- Gate finger (heating element) length: 1 μm
- Gate finger (heating element) width: 200 μm
- Gate/source, gate/drain spacing: 1 μm
- Source/drain finger length: 27 μm
- Si substrate thickness: 150 μm
- GaN thickness: 2.5 μm
- Backside Au layer thickness: 5 μm
- Die-attach thickness: 50 μm
- Source/drain metal Au thickness: 5 μm
- Gate metal Au thickness: 0.5 μm
- Via hole external diameter: 80 μm
- Via hole Au metal thickness: 5 μm
- Si thermal conductivity: $148*(300/T)^{1.3}$ W/(m*K)
- Si specific heat: 710 J/(kg*K)
- Si density: 2329 kg/m^3
- GaN thermal conductivity: $160*(300/T)^{1.4}$ W/(m*K)
- GaN specific heat: 490 J/(kg*K)
- GaN density: 6150 kg/m^3
- Die attach thermal conductivity: 45 W/(m*K)
- Die attach specific heat: 227 J/(kg*K)
- Die attach density: 7300 kg/m^3
- Au thermal conductivity: 318 W/(m*K)
- Au specific heat: 128 J/(kg*K)
- Au density: 19320 kg/m^3
- Thermal boundary resistance: $3.3*10^{-8}$ m^{2}K/W.

In all of the simulations shown here, the bottom of the die attach layer is isothermal at 300 K, so we are not considering the static and dynamic thermal influence of what follows the die attach in the heat flow path (e.g., package, heat sink). A surface drain pad is included (lower right corner of the surface in Fig. 1), where thermal boundary conditions are varied from isothermal (300 K) to adiabatic.

Fig. 3 shows an example of FE thermal simulation, obtained for a dissipated power of 0.5 W/finger (2.5 W/mm), with adiabatic drain pad (worst case).

LUMPED-ELEMENT MODELING

(1) Empirical LE modeling: Foster RC networks – We want to model the dynamic self-heating behavior of the structure in Fig. 1 with the Foster RC thermal network of Fig. 4. We start from the FE-simulated temperature response to a dissipated power step, which is fed to an algorithm that extracts a rough estimate of the relevant time constant from the peaks of the dT/(d(ln(t)) response [3] (T is the temperature of the hottest spot, t is time); an optimization algorithm then gets rid of the irrelevant time constants and fine-tunes the relevant ones. Fig. 5 shows the results.

The automated algorithm extracts 4 time constants, 2 of which are very similar, so the optimized Foster network has 3 RC stages, with τ_1 = 5.12 μs ($R_{\Theta 1}$ = 53.2 K/W, $C_{\Theta 1}$ = 9.60 10^{-8} J/K), τ_2 = 45.8 μs ($R_{\Theta 2}$ = 49.6 K/W, $C_{\Theta 2}$ = 9.25 10^{-7} J/K), τ_3 = 441 μs ($R_{\Theta 3}$ = 159 K/W, $C_{\Theta 3}$ = 2.77 10^{-6} J/K). It is to be noticed that, while Foster networks are handy because the time constants are given by the product of the resistance and capacitance of each stage, this approach yields a purely empirical model, where thermal R's and C's cannot be given a true physical meaning; it is also worth pointing out that the FE simulation features T-dependent thermal conductivities for GaN and Si. This example shows that the empirical LE Foster network approach can replicate the dynamics of self-heating with very good accuracy with as few as 3 RC stages.

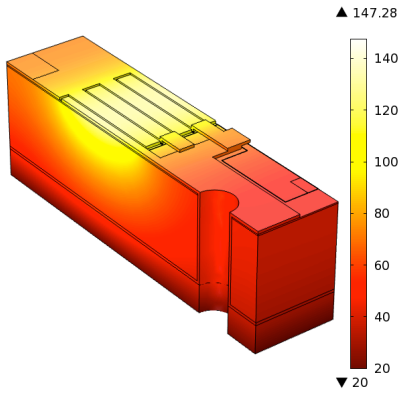

Fig. 3 FE thermal simulation of the structure of Fig. 1. P_D = 0.5 W/finger. Temperatures in °C.

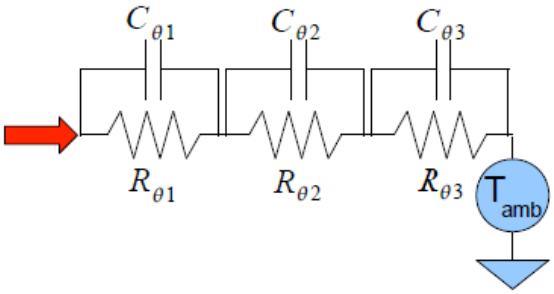

Fig. 4 3-stage LE Foster thermal network. The red arrow indicates the power inflow. T_{amb} is the ambient temperature.

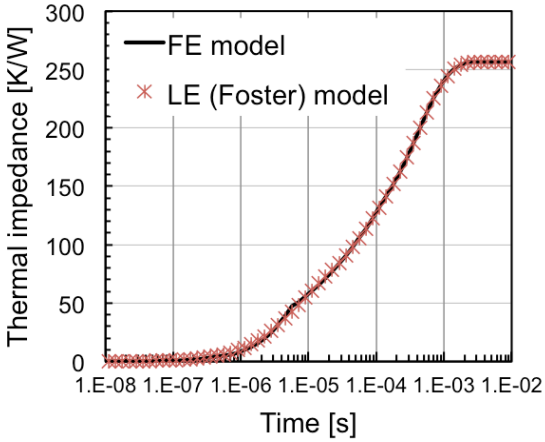

Fig. 5 Thermal impedance ($\Delta T(t)/P_D$) of a HEMT finger following a power step of P_D = 0.5 W/finger, as given by the FE simulation and the 3-stage LE Foster RC network. The temperature is that of the hottest spot of the HEMT.

This LE thermal modeling approach is relatively commonplace, with level of complexity starting from a single time constant (single RC stage), but it overlooks the fact that the whole HEMT structure is hardly characterized by a single, uniform temperature.

It turns out that finger-to-finger temperature differences are not dramatic in compact, wide-periphery structures made of numerous blocks like the one we are studying (Fig. 1). For example, in the case of P_D = 0.5 W/finger, the temperatures reached at the center of the hottest and coolest fingers of the structure in Fig. 1, as given by FE simulations, are 430.9 K and 429.0 K, respectively.

While this finger-to-finger temperature non-uniformity is not large enough to have a significant impact on the HEMT behavior, and therefore can be neglected in the development of the thermal model, the temperature variation along the finger width is quite another matter, as shown by Fig. 6.

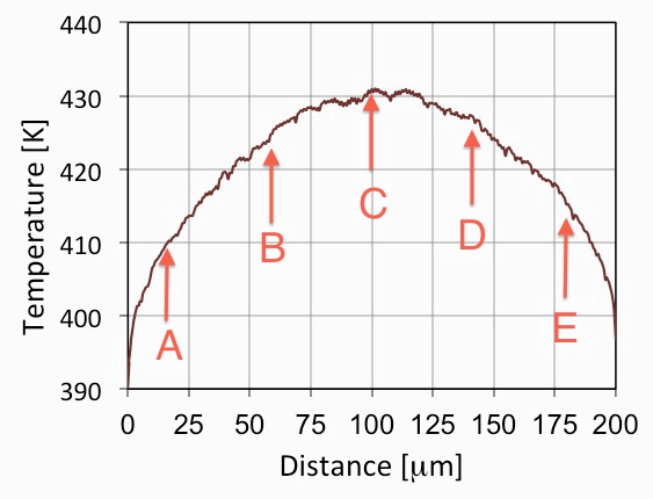

Fig. 6 Temperature distribution along the 200 μm width of the hottest (rightmost) finger of Fig. 1 and 2, as given by the FE simulation. P_D = 0.5 W/finger. Distance is measured from the finger edge closest to the source via hole. The arrows mark the points used for the extraction of the LE thermal networks. The ambient temperature is 300 K.

A temperature variation of about 40 K between the finger center and its edge, as shown by Fig. 6, cannot be neglected, which prevents the HEMT to be modeled as a 2D structure lying in the plane orthogonal to the finger width (as we did in [1]). We therefore partitioned the HEMT finger into 5 sections along the width dimension, each of them 40 μm-wide, and extracted the LE Foster networks from the temperature step response of the central point of each section (points marked A to E in Fig. 6). The match between the FE dynamic simulation and the response of the LE Foster networks is very good for all points A-E. Fig. 7 shows the comparison between FE and LE model for point A.

The parameters of the LE Foster networks extracted for the 5 locations shown in Fig. 6 are listed in Tab. I, while the corresponding time constants are given in Tab.II.

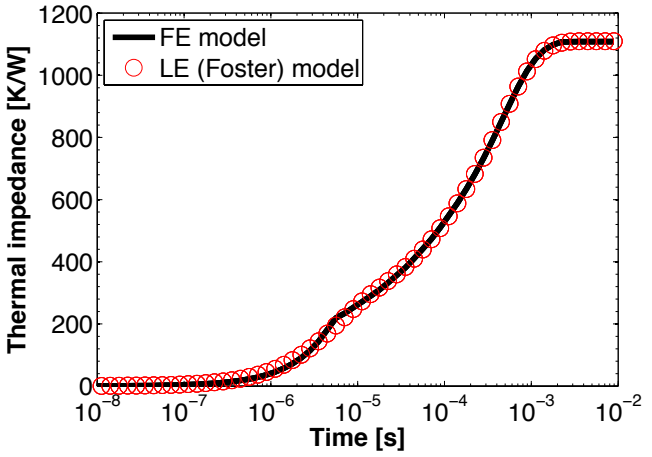

Fig. 7 Thermal impedance ($\Delta T(t)/P_D$) of point A (see Fig. 6) following a power step, applied to the 40 μm-wide element, of P_D = 0.1 W (0.5 W/finger), as given by the FE simulation and the 3-stage LE Foster RC network.

TABLE I
LE FOSTER RC THERMAL NETWORK PARAMETERS. P_D = 0.1 W IS INJECTED INTO EACH ELEMENT A-E

Point	Rθ1 [K/W]	Cθ1 [nJ/K]	Rθ2 [K/W]	Cθ2 [nJ/K]	Rθ3 [K/W]	Cθ3 [nJ/K]
A	249	19.8	162	315	698	647
B	267	19.2	227	207	760	582
C	266	19.2	248	185	794	555
D	262	19.6	215	207	796	555
E	247	19.9	136	326	769	582

It is worth pointing out that this LE description of the HEMT finger heating dynamics features 5 3-stage Foster networks, each representing an element of 40 μm of width in which we inject a 0.1 W dissipated power step: it is therefore quite reasonable that the values of thermal resistances of Tab. I are roughly 5 times, and the capacitances one fifth, of the values extracted from Fig. 5 for the whole finger.

TABLE II
LE FOSTER RC THERMAL NETWORK TIME CONSTANTS

Point	τ_1 [μs]	τ_2 [μs]	τ_3 [μs]
A	4.95	51.1	452
B	5.14	47.4	444
C	5.12	45.8	441
D	5.14	44.5	442
E	4.92	44.3	448

(2) LE modeling: Cauer RC networks – While the parameter values shown in Tables I and II make a lot of sense (including the fact that the time constants of Tab. II are nearly the same for the 5 locations A-E), the non-physical placement of the thermal capacitances in the Foster-type network prevents the possibility of attaching them a physical meaning, even in the framework of a gross

discretization of the physical distributed structure. On the other hand, a LE description of the thermal dynamics of the system that is more physics-based can be obtained using the Cauer-type RC network shown in Fig. 8 [3].

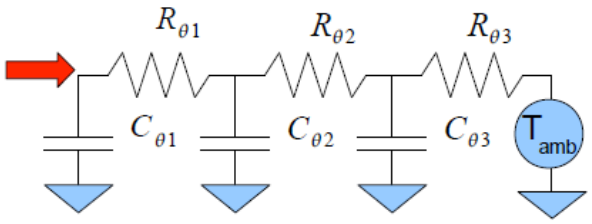

Fig. 8 3-stage LE Cauer thermal network. The red arrow indicates the power inflow. T_{amb} is the ambient temperature.

The drawback of Cauer networks is that the time constants are not easily calculated by multiplying the resistance and capacitance of each stage, as in Foster networks; consequently, direct extraction of the parameters (resistances and capacitances) is trickier, and the common approach is that of first extracting the Foster network from measured data (or FE simulations, as we do here), then converting the Foster network into a Cauer equivalent network using network theory formulas and algorithms [6].

Tab. III gives the parameters of the Cauer LE thermal networks (see Fig. 8) for points A-E. The match between the Foster and Cauer network behavior (not shown) is perfect.

TABLE III
LE CAUER RC THERMAL NETWORK PARAMETERS. P_D = 0.1 W IS INJECTED INTO EACH ELEMENT A-E

Point	RΘ1 [K/W]	CΘ1 [nJ/K]	RΘ2 [K/W]	CΘ2 [nJ/K]	RΘ3 [K/W]	CΘ3 [nJ/K]
A	297	18.1	310	226	504	603
B	336	17.1	356	164	568	569
C	341	16.9	370	149	598	545
D	331	17.3	341	163	601	525
E	294	18.2	286	226	572	494

The 5 Cauer (or Foster) networks defined by Tab. III (or Tab. II) represent therefore a simple yet accurate dynamic thermal model of a single HEMT finger, as summarized in Fig. 9. Should other fingers be modeled separately (it was shown above that this is unnecessary in our structure, due to modest finger-to-finger temperature non-uniformity), the same approach can be followed for each individual finger.

The dynamic thermal model of each finger section A-E may then be coupled to a temperature-dependent large-signal HEMT model [1], [2] to achieve self-consistent electro thermal modeling of the HEMT behavior.

CONCLUSIONS

This work shows results of dynamic lumped-element (LE) thermal modeling of power AlGaN/GaN HEMTs. A realistic 3D structure including top-side metals, thermal boundary resistance between GaN and substrate, die-attach, and source via hole is modeled using a finite-element (FE) tool, and the results are used to develop simple LE thermal models. We show that LE models with as few as 3 RC stages match the dynamic FE data with excellent accuracy.

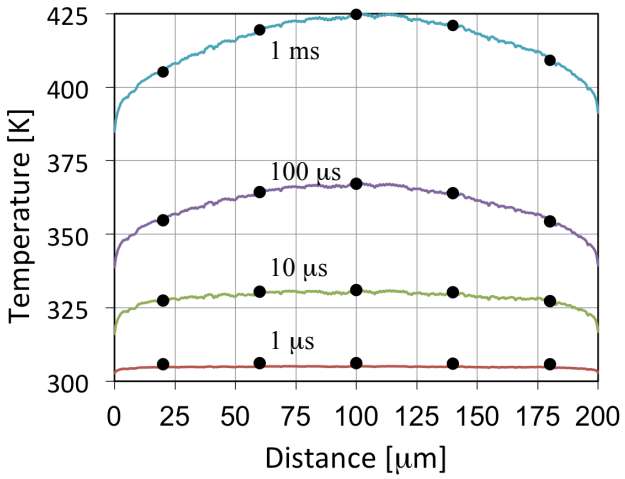

Fig. 9 Temperature distribution along the 200 µm width of the hottest (rightmost) finger of Fig. 1, as given by the FE simulation (solid lines) and LE models (dots), at different times following a power step P_D = 0.5 W/finger.

Further developments will be modeling the effect of different surface (e.g., heat dissipation through the surface drain pad) as well as backside (package, heat sink) thermal boundary conditions. While the former is unlikely to require modifications of the 3-stage topology of the LE networks, including the effect of package and heat sink will call for two additional RC stages to account for the much longer time constants associated with these massive elements. In the case of the Cauer representation, the thermal resistances and capacitances of package and heat-sink can be estimated from their geometries and material properties.

REFERENCES

[1] F. Bertoluzza et al., *IEEE Trans. Microw. Th. Techn.*, vol. 57, Dec. 2009, pp. 3163-3170.
[2] M. Bernardoni et al., *Proc. ESSDERC 2011*, pp. 171-174.
[3] V. Székely, *Microel. J.*, vol. 28, 1997, pp. 277-292.
[4] F. Bertoluzza et al., *Microel. Reliab.*, vol. 49, 2009, pp. 468-473.
[5] A. Sarua et al., *IEEE Trans. El. Dev.*, vol. 54, Dec. 2007, pp. 3152-3158.
[6] Y. C. Gerstenmaier et al., *Proc. THERMINIC 2007*, pp. 115-120.

ACRONYMS

HEMT: High Electron Mobility Transistor
PA: Power Amplifier
FE: Finite Element
LE: Lumped Element
TBR: Thermal Boundary Resistance